Table 3 Individual characteristics and outcomes

	Patient									
	1	2	3	4	5	6	7	8	9	10
Group A (750 mg q8h)										
Baseline characteristics										
Age/sex	60/F	42/M	53/F	47/M	46/M	47/M	54/M	46/F	62/F	44/M
Height (cm)	154.6	171.6	147.3	168.0	178.5	165.0	169.0	154.0	159.0	161.0
Weight (kg)	54.0	58.3	65.1	64.9	72.6	72.0	65.0	38.0	54.0	59.0
IL-28B SNP (rs8099917)	TT	TG	TT	TG	TT	TT	TT	TT	TT	TT
IL-28B SNP (rs12979860)	CC	CT	CC	CT	CC	CC	CC	CC	CC	CC
ITPA SNP (rs1127354)	CC	CC	CA	CC	CC	CC	CA	CC	CC	CC
Core a.a. 70 (W/M)	W	M	W	W	M	W	M	M	W	W
Core a.a. 91 (W/M)	W	W	W	W	W	W	W	W	W	M
ISDR substituted a.a. sites	0	0	1	0	0	0	0	1	1	1
History of IFN-based therapy†	IFN	IFN	Naïve	PR	Naïve	IFN	Naïve	Naïve	Naïve	Naïve
Baseline laboratory data										
HCV RNA (log_{10} IU/mL)	6.10	6.85	7.10	7.15	6.85	6.55	6.40	5.60	6.00	6.00
Hb (g/dL)	13.1	14.3	16.0	14.2	14.9	13.8	14.2	13.9	12.8	15.8
Creatinine (g/dL)	0.93	0.77	0.66	0.77	0.76	0.85	0.73	0.49	0.51	**0.83**
Dose										
RBV, max/min (mg)	600/400	600/200	800/200	800/200	800/400	800/200	800/200	600/200	600/200	600/200
Duration of treatment (weeks)	4	12	7	12	12	12	12	12	6	12
Telaprevir, adherence (%)	36.1	99.2	44.7	99.2	98.0	99.2	97.6	98.8	45.1	**101.6**
PEG IFN, adherence (%)	41.7	100	41.7	100	100	75.0	66.7	100	41.7	**100**
RBV, Adherence (%)	32.2	59.6	28.2	51.2	67.4	64.7	51.5	42.7	21.6	**45.1**
Pharmacokinetic parameter‡										
C_{trough} (μg/mL)	3.102	2.485	3.408	2.662	3.807	2.947	1.294	3.396	3.164	1.932
Outcome										
HCV RNA negativity (weeks)	2	6	2	4	4	4	4	6	2	2
Effect of therapy (SVR/BT/TR/NR)§	TR	TR	SVR	TR	SVR	TR	TR	TR	SVR	SVR

Table 3 *Continued*

	Patient									
	1	2	3	4	5	6	7	8	9	10
Group B (500 mg q8h)										
Baseline characteristics										
Age/sex	64/M	54/F	36/F	60/F	52/M	46/F	56/F	65/M	56/F	54/M
Height (cm)	173.2	151.0	148.7	160.5	175.8	160.0	160.0	167.0	158.0	170.0
Weight (kg)	75.0	47.6	44.3	67.9	71.8	52.0	57.0	79.0	65.0	55.0
IL-28B SNP (rs8099917)	TT	TG	TG	TT	TG	TT	TG	TT	TT	TG
IL-28B SNP (rs12979860)	CC	CT	CT	CC	CT	CC	CT	CC	CC	CT
ITPA SNP (rs1127354)	CC	CC	CC	CC	CC	CC	CC	CC	CC	CA
Core a.a. 70 (W/M)	M	W	W	W	M	W	M	W	W	M
Core a.a. 91 (W/M)	W	W	W	W	M	W	M	W	M	M
ISDR substituted a.a. sites	6	0	1	0	0	0	0	0	0	0
History of IFN-based therapy†	Naïve	IFN	Naïve	Naïve	PR	Naïve	PR	IFN	IFN	PR
Baseline laboratory data										
HCV RNA (log_{10} IU/mL)	5.50	7.15	6.15	6.80	6.80	7.00	6.10	7.20	6.85	6.75
Hb (g/dL)	16.1	11.7	12.1	13.6	14.5	12.3	16.8	14.3	13.7	14.8
Creatinine (g/dL)	0.78	0.50	0.45	0.56	0.87	0.58	0.80	0.89	0.75	0.70
Dose										
RBV, max/min (mg)	800/400	600/200	600/200	800/400	800/200	600/200	600/600	800/200	800/200	600/200
Duration of treatment (weeks)	12	12	11	12	12	3	12	12	5	12
Telaprevir, adherence (%)	98.0	99.2	91.0	99.2	101.6	25.5	98.8	99.2	43.1	98.4
PEG IFN, adherence (%)	98.3	66.7	87.5	100	91.7	25.0	100	100	41.7	100
RBV, adherence (%)	68.5	44.7	39.2	54.4	48.8	24.3	99.2	36.5	28.2	64.3
Pharmacokinetic parameter‡										
C_{trough} (μg/mL)	1.950	2.763	3.276	1.690	1.478	1.939	2.955	4.065	1.962	1.846
Outcome										
HCV RNA negativity (weeks)	2	6	2	2	4	-	2	2	2	8
Effect of therapy (SVR/BT/TR/NR)	SVR	TR	SVR	SVR	TR	NR	TR	SVR	SVR	TR

†Naïve, treatment naïve, IFN, IFN monotherapy, PR, PEG IFN/RBV.
‡Pharmacokinetic parameters of the patients who received triple therapy at weeks 2.
a.a., amino acid; ALT, alanine aminotransferase; C_{trough}, plasma trough concentrations; GGT, γ-glutamyltransferase; Hb, hemoglobin; HCV, hepatitis C virus; IFN, interferon; IL, interleukin; ISDR, interferon sensitivity-determining region; M, mutant; PEG, pegylated; Plt, platelets; RBV, ribavirin; SNP, single nucleotide polymorphism; SVR, sustained virological response, BT, breakthrough, TR, transient response, NR, non-response; W, wild type; WBC, white blood cell.

Table 4 Adverse events developing in more than 20% of patients in total

MedDRA/J (ver. 12.0) PT	Group A (750 mg q8h) $n = 10$ n (%)	Group B (500 mg q8h) $n = 10$ n (%)	Total $n = 20$ n (%)
Platelet count decreased	10 (100.0)	10 (100.0)	20 (100.0)
Anemia	10 (100.0)	9 (90.0)	19 (95.0)
White blood cell count decreased	9 (90.0)	10 (100.0)	19 (95.0)
Rash	7 (70.0)	7 (70.0)	14 (70.0)
Pyrexia	6 (60.0)	8 (80.0)	14 (70.0)
Malaise	6 (60.0)	5 (50.0)	11 (55.0)
Blood triglycerides increased	6 (60.0)	5 (50.0)	11 (55.0)
Headache	3 (30.0)	7 (70.0)	10 (50.0)
Blood lactate dehydrogenase increased	3 (30.0)	7 (70.0)	10 (50.0)
Anorexia	3 (30.0)	6 (60.0)	9 (45.0)
Blood uric acid increased	4 (40.0)	4 (40.0)	8 (40.0)
Nausea	3 (30.0)	5 (50.0)	8 (40.0)
Pruritus	3 (30.0)	5 (50.0)	8 (40.0)
Protein total decreased	0 (0.0)	8 (80.0)	8 (40.0)
Hyperuricaemia	5 (50.0)	2 (20.0)	7 (35.0)
Blood creatinine increased	5 (50.0)	2 (20.0)	7 (35.0)
Nasopharyngitis	3 (30.0)	4 (40.0)	7 (35.0)
Neutrophil percentage decreased	3 (30.0)	4 (40.0)	7 (35.0)
Influenza-like illness	4 (40.0)	2 (20.0)	6 (30.0)
Abdominal discomfort	2 (20.0)	3 (30.0)	5 (25.0)
Vomiting	2 (20.0)	3 (30.0)	5 (25.0)
Dizziness	0 (0.0)	5 (50.0)	5 (25.0)
Dysgeusia	3 (30.0)	1 (10.0)	4 (20.0)
Stomatitis	3 (30.0)	1 (10.0)	4 (20.0)
Lymphocyte percentage increased	2 (20.0)	2 (20.0)	4 (20.0)
Diarrhea	1 (10.0)	3 (30.0)	4 (20.0)
Alopecia	1 (10.0)	3 (30.0)	4 (20.0)

contrary, there was observed a difference in serum creatinine concentrations between group A and group B; thus, the serum creatinine concentrations in group A were higher than those in group B at all of the time points examined with a statistical significance at weeks 4 and 8 ($P < 0.01$ and $P < 0.05$, respectively) as shown in Figure 2(b). The TVR Review Team confirms that higher exposure of TVR and RBV was significantly associated with increased risk of anemia and grade 2 or higher hemoglobin toxicity.[11] The behaviors of hemoglobin and creatinine in the triple therapy shown in Figure 2 are of interest from the viewpoints of development of anemia with TVR-based regimen and could be explained by the following possibilities: (i) the increase of plasma concentration of TVR may directly affect the renal function to cause the increase of creatinine especially in group A and the decrease of hemoglobin; (ii) TVR first caused the increase of systemic exposure to RBV which in turn additively or synergistically resulted in renal dysfunction. The decrease of renal function reportedly leads to the increase of RBV concentration in plasma, because RBV is mainly excreted via the renal route.[24,25] In this study, the AUC_{0-8h} on day 1 of patients who developed low hemoglobinemia (<8.5 g/dL) were significantly higher than those of the other patients. The pharmacokinetic parameters of TVR on day 14, at which plasma concentrations of TVR were in the steady state, did not affect low hemoglobinemia. The timing of reducing RBV dose may cause development of low hemoglobinemia, because the RBV dose reduction set in the protocol of this study was less strict than that in the previous reports.[7,8]

Because the present data show that the TVR exposure tended to be increased in a dose-dependent manner, there is a possibility that the triple therapy with TVR 500 mg q8h is advantageous in aged patients whose renal function, body water content or both are lower than those of younger patients. It should be noted,

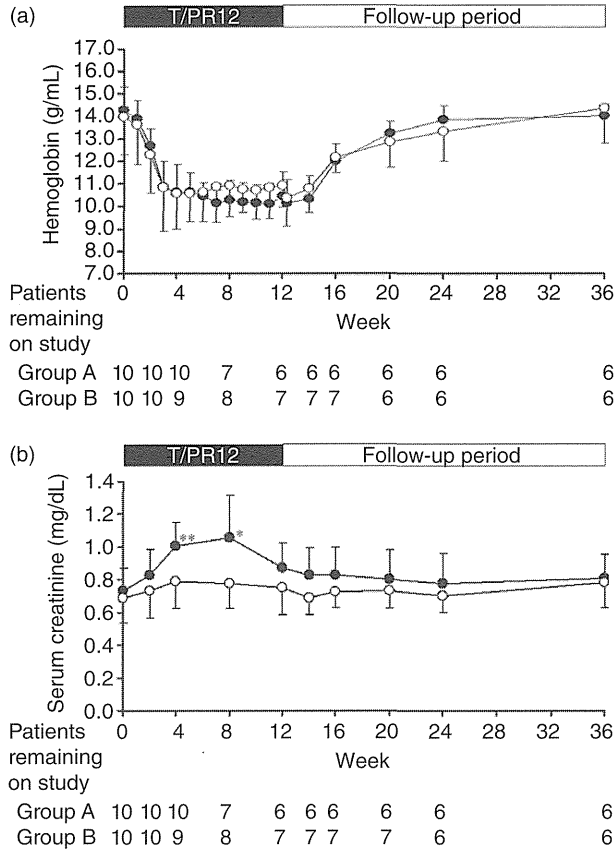

Figure 2 (a) Change from baseline of hemoglobin and (b) serum creatinine levels in Japanese patients with chronic hepatitis C during the telaprevir-based triple therapy. Each circle and bar represent mean values ± standard deviations, respectively. Number of patients at each time point is indicated below. Statistical tests were performed at each point. $*P < 0.05$ and $**P < 0.01$ difference. —●—, Group A (telaprevir 750 mg q8h); —○—, group B (telaprevir 500 mg q8h). T/PR12, triple therapy of telaprevir with peginterferon and ribavirin for 12 weeks.

however, that the small number of patients per arm in this study limits conclusions that can be drawn, and a future larger study is essential.

In conclusion, although the exposure to TVR tended to be lower in 500 mg q8h than that in 750 mg q8h in the TVR-based triple therapy, relatively high exposure of TVR was observed in Japanese CHC patients given TVR at the lower dose. The result suggests that the lower dose regimen may be one of the options for the treatment of Japanese patients. In addition, in the view of antiviral effects, TVR pharmacokinetics and safety profiles, the present findings indicate that development of adverse events, specifically anemia and creatinine increase in the treatment with TVR-based regimen, could be avoided by dose adjustment of TVR as well as RBV.

ACKNOWLEDGMENT

THIS STUDY WAS supported in part by a Grant-in-Aid from the Ministry of Health, Labor and Welfare of Japan.

REFERENCES

1 World Health Organization. *Hepatitis C. (Global Alert and Response, 2002)*. Geneva: World Health Organization, 2002; Updated February 2010. Available at: http://www.who.int/mediacentre/factsheets/fs164/en/. Accessed October, 2012.
2 Hoofnagle JH. Course and outcome of hepatitis C. *Hepatology* 2002; **36:** S21–S29.
3 Seeff LB. Natural history of chronic hepatitis C. *Hepatology* 2002; **36:** S35–46.
4 Jacobson IM, McHutchison JG, Dusheiko G *et al.* Telaprevir for previously untreated chronic hepatitis C virus infection. *N Engl J Med* 2011; **364:** 2405–16.
5 Zeuzem S, Andreone P, Pol S *et al.* Telaprevir for retreatment of HCV infection. *N Engl J Med* 2011; **364:** 2417–28.
6 Sherman KE, Flamm SL, Afdhal NH *et al.* Response-guided telaprevir combination treatment for hepatitis C virus infection. *N Engl J Med* 2011; **365:** 1014–24.
7 Kumada H, Toyota J, Okanoue T, Chayama K, Tsubouchi H, Hayashi N. Telaprevir with peginterferon and ribavirin for treatment-naive patients chronically infected with HCV of genotype 1 in Japan. *J Hepatol* 2012; **56:** 78–84.
8 Hayashi N, Okanoue T, Tsubouchi H, Toyota J, Chayama K, Kumada H. Efficacy and safety of Telaprevir, a new protease inhibitor, for difficult-to-treat patients with genotype 1 chronic hepatitis C. *J Viral Hepat* 2012; **19:** 134–42.
9 Hezode C, Forestier N, Dusheiko G *et al.* Telaprevir and peginterferon with or without ribavirin for chronic HCV infection. *N Engl J Med* 2009; **360:** 1839–50.
10 Reesink HW, Zeuzem S, Weegink CJ *et al.* Rapid decline of viral RNA in hepatitis C patients treated with VX-950: a phase Ib, placebo-controlled, randomized study. *Gastroenterology* 2006; **131:** 997–1002.
11 Antiviral Products Advisory Committee. Telaprevir NDA briefing document. Available at: http://www.fda.gov/downloads/AdvisoryCommittees/CommitteesMeetingMaterials/Drugs/AntiviralDrugsAdvisoryCommittee/UCM252561. Accessed October, 2012.
12 Telaprevir NDA 201-917 vertex pharmaceuticals. FDA Advisory Committee Briefing.Document. Available at: http://www.fda.gov/downloads/AdvisoryCommittees/CommitteesMeetingMaterials/Drugs/AntiviralDrugsAdvisoryCommittee/UCM252562. Accessed October, 2012.

13 Suzuki F, Akuta N, Suzuki Y *et al.* Rapid loss of hepatitis C virus genotype 1b from serum in patients receiving a triple treatment with telaprevir (MP-424), pegylated interferon and ribavirin for 12 weeks. *Hepatol Res* 2009; **39**: 1056–63.
14 Akuta N, Suzuki F, Sezaki H *et al.* Association of amino acid substitution pattern in core protein of hepatitis C virus genotype 1b high viral load and non-virological response to interferon-ribavirin combination therapy. *Intervirology* 2005; **48**: 372–80.
15 Akuta N, Suzuki F, Kawamura Y *et al.* Predictive factors of early and sustained responses to peginterferon plus ribavirin combination therapy in Japanese patients infected with hepatitis C virus genotype 1b: amino acid substitutions in the core region and low-density lipoprotein cholesterol levels. *J Hepatol* 2007; **46**: 403–10.
16 Enomoto N, Sakuma I, Asahina Y *et al.* Comparison of full-length sequences of interferon sensitive and resistant hepatitis C virus 1b. Sensitivity to interferon is confered by amino acid substitutions in the NS5A region. *J Clin Invest* 1995; **96**: 224–30.
17 Enomoto N, Sakuma I, Asahina Y *et al.* Mutations in the nonstructural protein 5A gene and response to interferon in patients with chronic hepatitis C virus 1b infection. *N Engl J Med* 1996; **334**: 77–81.
18 Ohnishi Y, Tanaka T, Ozaki K, Yamada R, Suzuki H, Nakamura Y. A high-throughput SNP typing system for genome-wide association studies. *J Hum Genet* 2001; **46**: 471–7.
19 Suzuki A, Yamada R, Chang X *et al.* Functional haplotypes of PADI4, encoding citrullinating enzyme peptidylarginine deiminase 4, are associated with rheumatoid arthritis. *Nat Genet* 2003; **34**: 395–402.
20 Suzuki F, Suzuki Y, Akuta N *et al.* Influence of *ITPA* polymorphism on decreases of hemoglobin during treatment with pegylated IFN, ribavirin and telaprevir. *Hepatology* 2011; **53**: 415–21.
21 Marcellin P, Forns X, Goeser T *et al.* Telaprevir is effective given every 8 or 12 hours with ribavirin and peginterferon alfa-2a or 2b to patients with chronic hepatitis C. *Gastroenterology* 2011; **140**: 459–68.
22 Chayama K, Hayes CN, Abe H *et al.* IL28B but not ITPA polymorphism is predictive of response to pegylated interferon, ribavirin, and telaprevir triple therapy in patients with genotype 1 hepatitis C. *J Infect Dis* 2011; **204**: 84–93.
23 Akuta N, Suzuki F, Miharu M *et al.* Amino acid substitution in hepatitis C virus core region and genetic variation near the interleukin 28B gene predict viral response to telaprevir with peginterferon and ribavirin. *Hepatology* 2010; **57**: 421–9.
24 Maeda Y, Kiribayashi Y, Moriya T *et al.* Dosage adjustment of ribavirin based on renal function in Japanese patients with chronic hepatitis C. *Ther Drug Monit* 2004; **26**: 9–15.
25 Toyoda H, Kumada T, Kiriyama S *et al.* Correlation of serum ribavirin concentration with pretreatment renal function estimates in patients with chronic hepatitis C receiving combination antiviral therapy with peginterferon and ribavirin. *J Viral Hepat* 2008; **15**: 651–8.

Journal of Medical Virology 85:1028–1036 (2013)

Emergence of Telaprevir-Resistant Variants Detected by Ultra-Deep Sequencing After Triple Therapy in Patients Infected With HCV Genotype 1

Norio Akuta,[1]* Fumitaka Suzuki,[1] Yuya Seko,[1] Yusuke Kawamura,[1] Hitomi Sezaki,[1] Yoshiyuki Suzuki,[1] Tetsuya Hosaka,[1] Masahiro Kobayashi,[1] Tasuku Hara,[1] Mariko Kobayashi,[2] Satoshi Saitoh,[1] Yasuji Arase,[1] Kenji Ikeda,[1] and Hiromitsu Kumada[1]

[1]*Department of Hepatology, Toranomon Hospital, and Okinaka Memorial Institute for Medical Research, Tokyo, Japan*

[2]*Liver Research Laboratory, Toranomon Hospital, Tokyo, Japan*

Using ultra-deep sequencing technology, the present was designed to investigate whether the emergence of telaprevir-resistant variants (amino acid substitutions of aa36, aa54, aa155, aa156, and aa170 positions in HCV NS3 region) after commencement of triple therapy of telaprevir/peginterferon (PEG-IFN)/ribavirin could be predicted at baseline in previous non-responders to dual therapy. Fourteen patients infected with HCV genotype 1 who did not respond to previous PEG-IFN/ribavirin, received a 24-week regimen of triple therapy, and were evaluated for appearance of telaprevir-resistant variants (amino acid substitutions of more than 0.2% among the total coverage) by ultra-deep sequencing. The sustained virological response rate was 28.6% (4 of 14 patients), which was significantly higher in patients with Arg70 (substitution at core aa70) and partial response (type of previous response to PEG-IFN/ribavirin) than in other patients. Telaprevir-resistant variants at baseline were detected in 7.1% (1 of 14 patients) by direct sequencing and in 21.4% (3 of 14 patients) by ultra-deep sequencing. The appearance of telaprevir-resistant variants was examined by ultra-deep sequencing in 10 who did not show sustained virological responders. De novo variants emerged at re-elevation of viral load, regardless of variant frequencies at baseline (one patient with very high frequency variants [T54S: 99.9%], two patients with very low frequency variants [V36A: 0.2%; and V170A: 0.4%], and seven patients of undetectable variants). It is concluded that it is difficult to predict at baseline the emergence of telaprevir-resistant variants after commencement of triple therapy in prior non-responders of HCV genotype 1, even with the use of ultra-deep sequencing. ***J. Med. Virol. 85:1028–1036, 2013.***

KEY WORDS: HCV; ultra-deep sequence; telaprevir; resistant variants; non-response

INTRODUCTION

New strategies have been introduced for the treatment of chronic hepatitis C virus (HCV) infection based on inhibition of protease in the NS3/NS4 of the HCV polyprotein. Of these, telaprevir (VX-950) was selected as a candidate agent for treatment of chronic HCV infection [Lin et al., 2006]. Three studies (PROVE1, PROVE2, and Japanese study) showed that a 24-week regimen of triple therapy (telaprevir, peginterferon [PEG-IFN], and ribavirin) for 12 weeks followed by dual therapy (PEG-IFN and ribavirin) for 12 weeks (also called the T12PR24 regimen) achieved sustained virological response (lasting more than 24 weeks after withdrawal of treatment) rates of 61%, 69%, and 73%, respectively, in patients infected with HCV genotype 1 (HCV-1) [Hézode et al., 2009; McHutchison et al., 2009; Kumada et al., 2012]. However, a recent study (PROVE3) showed lower sustained virological response rates for the T12PR24 regimen (39%) in non-responders to previous PEG-IFN/ribavirin therapy infected with HCV-1, who did not achieve HCV-RNA negativity during or at the

Grant sponsor: Ministry of Health, Labor and Welfare, Government of Japan; Grant sponsor: Ministry of Education Culture Sports Science and Technology, Government of Japan.

*Correspondence to: Norio Akuta, MD, Department of Hepatology, Toranomon Hospital, 2-2-2 Toranomon, Minato-ku, Tokyo 105-0001, Japan. E-mail: akuta-gi@umin.ac.jp

Accepted 30 January 2013
DOI 10.1002/jmv.23579
Published online in Wiley Online Library (wileyonlinelibrary.com).

end of the initial combination therapy [McHutchison et al., 2010]. Furthermore, telaprevir-based regimen is reported to induce resistant variants [Lin et al., 2005; Kieffer et al., 2007]. Thus, there is a need to determine the predictive factors for non-response to triple therapy before administration of such treatment in order to avoid the appearance of telaprevir-resistant variants.

Though Sanger sequencing has been used to determine viral sequences, ultra-deep sequencing technology is much faster and can perform large-scale sequencing. Recent reports have indicated that ultra-deep sequencing technology provides a better understanding of the dynamics of variants in HCV quasispecies [Bull et al., 2011; Hiraga et al., 2011; Nasu et al., 2011; Ninomiya et al., 2012]. However, it is not clear at this stage whether this can be useful to predict treatment response and treatment resistant variants, including telaprevir-resistant variants by triple therapy.

The aim of this study using ultra-deep sequencing technology was to investigate whether the presence of low frequency resistant variants at baseline could predict the emergence of telaprevir-resistant variants after the start of telaprevir/PEG-IFN/ribavirin triple therapy, in adult Japanese patients infected with HCV-1 who did not respond to previous PEG-IFN/ribavirin dual therapy.

PATIENTS AND METHODS

Study Patients

Between May 2008 and September 2009, 61 patients infected with HCV were recruited in this study at the Department of Hepatology, Toranomon Hospital, which is located in Metropolitan Tokyo. The study protocol was in compliance with the Good Clinical Practice Guidelines and the 1975 Declaration of Helsinki, and was approved by the institutional review board. Each patient gave an informed consent before participation in this trial. Patients were assigned to a 24-week regimen of triple therapy (telaprevir [MP-424], PEG-IFN and ribavirin) for 12 weeks followed by dual therapy of PEG-IFN and ribavirin for 12 weeks (the T12PR24 regimen).

Fourteen of the 61 patients met the following inclusion and exclusion criteria: (1) diagnosis of chronic hepatitis C. (2) HCV-1b confirmed by sequence analysis. (3) HCV RNA levels of $\geq$5.0 log IU/ml determined by the COBAS TaqMan HCV test (Roche Diagnostics, Tokyo, Japan). (4) Japanese (Mongoloid) ethnicity. (5) Age at study entry of 20–65 years. (6) Body weight $\geq$35 and $\leq$120 kg at the time of registration. (7) Absence of decompensated cirrhosis of the liver. (8) No detectable hepatitis B surface antigen in serum. (9) No history of hepatocellular carcinoma. (10) No previous treatment for malignancy. (11) No history of autoimmune hepatitis, alcohol liver disease, hemochromatosis, or chronic liver disease other than chronic hepatitis C. (12) No history of depression, schizophrenia or suicide attempts, hemoglobinopathies, angina pectoris, cardiac insufficiency, myocardial infarction or severe arrhythmia, uncontrollable hypertension, chronic renal dysfunction or creatinine clearance of $\leq$50 ml/min at baseline, diabetes requiring treatment or fasting glucose level of $\geq$110 mg/dl, autoimmune disease, cerebrovascular disorders, thyroid dysfunction uncontrollable by medical treatment, chronic pulmonary disease, allergy to medication or anaphylaxis at baseline. (13) Hemoglobin level of $\geq$12 g/dl, neutrophil count $\geq$1,500/mm^3, and platelet count of $\geq$100,000/mm^3 at baseline. Pregnant or breast-feeding women or those willing to become pregnant during the study and men with a pregnant partner were excluded from the study. (14) Prior non-responders, who did not achieve HCV-RNA negativity during or at the end of 24- to 48-week PEG-IFN plus ribavirin combination therapy.

Non-response to previous therapy was defined as null response (a reduction of less than 2 $\log_{10}$ in HCV RNA during treatment) or partial response (a reduction of 2 $\log_{10}$ or more in HCV RNA during treatment). Table I summarizes the profiles and laboratory data of the 14 patients at commencement of treatment with the T12PR24 regimen. The study patients included seven males and seven females, aged 40–65 years (median, 56 years).

All 14 patients were followed-up for at least 24 weeks after the completion of treatment. The efficacy of treatment was evaluated by HCV-RNA negativity at 24 weeks after the completion of therapy (sustained virological response), based on the COBAS TaqMan HCV test (Roche Diagnostics). Furthermore, failure to achieve sustained virological response was classified as non-response (HCV-RNA detected during or at the end of treatment), viral breakthrough (re-elevation of viral loads before the end of treatment, even when HCV-RNA was temporarily negative during treatment), and relapse (re-elevation of viral loads after the end of treatment, even when HCV-RNA was negative at the end of treatment).

Telaprevir (MP-424; Mitsubishi Tanabe Pharma, Osaka, Japan) was administered at 750 mg three times a day at an 8-hr (q8) interval after the meal. PEG-IFNα-2b (PEG-Intron; Schering Plough, Kenklworth, NJ) was injected subcutaneously at a median dose of 1.5 μg/kg (range: 1.3–1.7 μg/kg) once a week. Ribavirin (Rebetol; Schering Plough) was administered at 200–600 mg twice a day after breakfast and dinner (daily dose: 600–1,000 mg). PEG-IFN and ribavirin were discontinued or their doses reduced, as required, upon reduction of hemoglobin level, leukocyte count, neutrophil count or platelet count, or the development of adverse events. Thus, the dose of PEG-IFN was reduced by 50% when the leukocyte count decreased below 1,500/mm^3, neutrophil count below 750/mm^3 or platelet count below 80,000/mm^3; PEG-IFN was discontinued when these counts decreased below 1,000/mm^3, 500/mm^3, or 50,000/mm^3, respectively. When hemoglobin decreased to $<$10 g/dl, the daily dose of ribavirin was reduced from 600 to 400 mg, from 800 to 600 mg,

TABLE I. Profile and Laboratory Data at Commencement of Telaprevir, Peginterferon and Ribavirin Triple Therapy of 14 Japanese Patients Infected With HCV Genotype 1b, Who Did Not Respond to Previous Peginterferon Plus Ribavirin Combination Therapy

Demographic data	
Number of patients	14
HCV genotype 1b	14
Japanese (Mongoloid) ethnicity	14
Sex (male/female)	7/7
Age (years)*	56 (40–65)
History of blood transfusion	3 (21.4%)
Family history of liver disease	2 (14.3%)
Body mass index (kg/m^2)*	23.0 (18.1–26.5)
Laboratory data	
Level of viremia (log IU/ml)	6.7 (5.8–7.4)
Serum aspartate aminotransferase (IU/L)	35 (20–108)
Serum alanine aminotransferase (IU/L)	45 (17–135)
Serum albumin (g/dl)	3.9 (3.4–4.5)
Gamma-glutamyl transpeptidase (IU/L)	50 (20–154)
Leukocyte count ($/mm^3$)	4,500 (3,300–6,500)
Hemoglobin (g/dl)	14.5 (12.6–16.6)
Platelet count ($\times 10^4/mm^3$)	16.2 (10.4–23.9)
Alpha fetoprotein (μg/L)	7 (2–38)
Total cholesterol (mg/dl)	180 (132–228)
Fasting plasma glucose (mg/dl)	89 (81–102)
Treatment	
PEG-IFNα-2b dose (μg/kg)	1.5 (1.3–1.7)
Ribavirin dose (mg/kg)	11.7 (8.1–14.5)
Amino acid substitutions in the HCV genotype 1b	
Core aa 70 (arginine/glutamine (histidine))	6/8
Core aa 91 (leucine/methionine)	6/8
ISDR of NS5A (wild-type/non wild-type)	13/1
IL28B genotype	
rs8099917 genotype (TT/TG/GG)	1/11/2
Type of previous response to peginterferon/ribavirin	
Partial response/null response	8/6

ND, not determined.
Data are number and percentages of patients.
*Median (range) values.

and from 1,000 to 600 mg, depending on the initial dose. Ribavirin was withdrawn when hemoglobin decreased to <8.5 g/dl. However, the dose of telaprevir (MP-424) remained the same, and its administration was stopped only when the discontinuation was considered appropriate for the development of adverse events. In those patients in whom telaprevir was discontinued, treatment with PEG-IFNα-2b and ribavirin was also terminated.

Measurement of HCV RNA

The antiviral effects of the triple therapy on HCV were assessed by measuring plasma HCV RNA levels. In this study, HCV RNA levels during treatment were evaluated at least once every month before, during, and after therapy. HCV RNA concentrations were determined using the COBAS TaqMan HCV test (Roche Diagnostics). The linear dynamic range of the assay was 1.2–7.8 log IU/ml, and the undetectable samples were defined as negative.

Assessment of Telaprevir-Resistant Variants

The genome sequence of the *N*-terminal 609 nucleotides (203 amino acids) in the NS3 region of HCV isolates from the patients was examined before, during, and after triple therapy. HCV RNA was extracted from 100 μl of serum and the nucleotide sequences were determined by direct sequencing and deep sequencing. The primers used to amplify the NS3 region were NS3-F1 (5′-ACA CCG CGG CGT GTG GGG ACA T-3′; nucleotides 3295–3316) and NS3-AS2 (5′-GCT CTT GCC GCT GCC AGT GGG A-3′; nucleotides 4040–4019) as the first (outer) primer pair and NS3-F3 (5′-CAG GGG TGG CGG CTC CTT-3′; nucleotides 3390–3407) and NS3-AS2 as the second (inner) primer pair [Akuta et al., 2012a,b; Suzuki et al., 2012]. Thirty-five cycles of first and second amplifications were performed as follows: denaturation for 30 sec at 95°C, annealing of primers for 1 min at 63°C, extension for 1 min at 72°C, and final extension was performed at 72°C for 7 min. The PCR-amplified DNA was purified after agarose gel electrophoresis, and then used for direct sequencing and deep sequencing.

All patients were tested at baseline. The analysis was also repeated at the time of re-elevation of viral loads in those patients who did not achieve sustained virological response. Telaprevir-resistant variants included V36A/C/M/L/G, T54A/S, R155K/T/I/M/G/L/S/Q, A156V/T/S/I/G, V170A [Barbotte et al., 2010; Romano et al., 2010].

Direct sequencing was analyzed by standard Sanger sequencing. Dideoxynucleotide termination sequencing was performed with the Big Dye Deoxy Terminator v1.1 Cycle Sequencing kit (Life Technologies, Carlsbad, CA) [Akuta et al., 2012a,b; Suzuki et al., 2012]. On the other hand, ultra-deep sequencing was performed using the Ion Personal Genome Machine (PGM) Sequencer (Life Technologies). An Ion Torrent adapter-ligated library was prepared using an Ion Xpress Plus Fragment Library Kit (Life Technologies). Briefly, 100 ng of fragmented genomic DNA was ligated to the Ion Torrent adapters P1 and A. The adapter-ligated products were nick-translated and PCR-amplified for a total of eight cycles. Subsequently, the library was purified using AMPure beads (Beckman Coulter, Brea, CA) and the concentration determined using the StepOne Plus RealTime PCR (Life Technologies) and Ion Library Quantitation Kit, according to the instructions provided by the manufacturer. Emulsion PCR was performed using Ion OneTouch (Life Technologies) in conjunction with Ion OneTouch 200 Template Kit v2 (Life Technologies). Enrichment for templated Ion spheres particles (ISPs) was performed using Ion OneTouch Enrichment System (Life Technologies), according to the instructions provided by the manufacturer. Templated ISPs was loaded onto an Ion 314 chip, and subsequently sequenced using 130 sequencing cycles according to the Ion PGM 200 Sequencing Kit user guide. Total output read length per run is over 10 Mbase (0.5M-tag, 200 base read) [Elliott et al., 2012]. The results were analyzed with the CLC Genomics Workbench software (CLCbio, Aarhus, Denmark) [Vogel et al., 2012].

A control experiment was included to validate the error rates in ultra-deep sequencing of the viral genome. In this study, amplification products of the second-round PCR were ligated with plasmid and transformed in *Escherichia coli* in a cloning kit (TA Cloning; Invitrogen, Carlsbad, CA). A plasmid-derived NS3 sequence was determined as the template, by the control experiment. The numbers of coverage evaluated per position for aa36, aa54, aa155, aa156, and aa170 in NS3 region, were 359379, 473716, 106435, 105979, and 49058, respectively. Thus, using the control experiment based on plasmid encoding HCV NS3 sequence, amino acid mutations were defined as amino acid substitutions at frequency of more than 0.2% among the total coverage. This frequency ruled out putative errors caused by deep sequence platform used in this study (Table II).

Detection of Amino Acid Substitutions in Core, and NS5A Regions of HCV-1b

With the use of HCV-J (accession no. D90208) as a reference [Kato et al., 1990], the sequence of 1–191 aa in the core protein of HCV-1b was determined and then compared with the consensus sequence constructed in a previous study to detect substitutions at aa 70 of arginine (Arg70) or glutamine/histidine (Gln70/His70) and aa 91 of leucine (Leu91) or methionine (Met91) [Akuta et al., 2005, 2007, 2012a,b]. The sequence of 2,209–2,248 aa in the NS5A of HCV-1b (ISDR) reported by Enomoto et al. [1996] was determined, and the numbers of aa substitutions in ISDR were defined as wild-type (0, 1) or non wild-type ($\geq$2) in comparison with HCV-J. In the present study, aa substitutions of the core region, and NS5A-ISDR of HCV-1b were analyzed by direct sequencing.

Determination of *IL28B* Genotype

IL28B (rs8099917 and rs12979860) were genotyped by the Invader assay, TaqMan assay, or direct sequencing, as described previously [Ohnishi et al., 2001; Suzuki et al., 2003].

Statistical Analysis

Non-parametric tests (chi-squared test and Fisher's exact probability test) were used to determine those factors that significantly contributed to sustained virological response and end-of-treatment response. All *P*-values less than 0.05 by the two-tailed test were considered significant. Variables that achieved statistical significance ($P < 0.05$) or marginal significance ($P < 0.10$) on univariate analysis were determined. For statistical analysis, each variable was transformed into categorical data consisting of two simple ordinal numbers. The potential pretreatment factors associated with sustained virological response included the following variables: sex, age, body mass index, HCV RNA level, type of previous response to PEG-IFN/ribavirin, *IL28B* genotype, and amino acid substitution in the core region/NS5A-ISDR.

TABLE II. Error Rates of Ultra-Deep Sequencing for the Plasmid Encoding HCV NS3 Sequence, Determined by the Control Experiment

Position	Coverage	Frequencies (%)	Error rates (%)[a]
aa36	359,415	V (99.9%), A/F/I (0.1%)	0.1
aa54	473,716	T (99.9%), A/I (0.1%)	0.1
aa155	106,435	R (99.9%), Q/W (0.1%)	0.1
aa156	105,979	A (99.9%), T/V (0.1%)	0.1
aa170	49,058	V (99.9%), A/I (0.1%)	0.1

[a]Amino acid mutations were defined as amino acid substitutions at a frequency of more than 0.2% among the total coverage. This frequency ruled out putative errors caused by deep sequence platform used in this study.

Statistical analysis was performed using the Statistical Package for Social Sciences (SPSS, Inc., Chicago, IL).

RESULTS

Virological Response to Therapy

Table III summarizes the profiles and laboratory data of the 14 patients at commencement of triple therapy, virological course, and efficacy of treatment. The sustained virological response rate was 28.6% (four patients [Cases 1–4]). Of the 10 patients (Cases 5–14) who did not show sustained virological response, the relapse, breakthrough and non-response rates were 50.0% (five patients [Cases 5–9]), 40.0% (4 [Cases 10–13]), and 10.0% (one [Cases 14]), respectively. Two patients (Cases 10, 13) stopped telaprevir before the completion of 12-week treatment (PEG-IFN and ribavirin continued), and one patient (Case 9) stopped the triple therapy at 9 weeks before the completion of the 24-week regimen, due to a fall in Hb concentration.

Thirteen of 14 patients showed *IL28B* rs8099917 non-TT and rs12979860 non-CC, whereas the other one patient (Case 4) had rs8099917 TT and rs12979860 CC. Thus, in non-responders to previous treatment, *IL28B* genotype did not play a role in sustained virological response. The sustained virological response rate was significantly higher in patients with Arg70 (66.7% [four of six patients]) than in those with Gln70(His70) (0% [zero of eight]; $P = 0.015$). Furthermore, the rate tended to be higher in patients with partial response to previous treatment (50.0% [four of eight patients]) than those with null response (0% [zero of six]; $P = 0.085$). Especially, the sustained virological response rate was significantly higher in patients with Arg70 plus partial response (80.0% [four of five patients]) than in other patients (0% [zero of nine]; $P = 0.005$). Thus, all four patients (100%) who achieved sustained virological response had Arg70 and showed partial response (Table III).

Detection of Telaprevir-Resistant Variants by Direct and Ultra-Deep Sequencing

Baseline telaprevir-resistant variants were detected by direct sequencing in 7.1% (one patient [Case 12 with T54S]), and by ultra-deep sequencing in 21.4% (three patients [Case 9 with V170A: 0.4% of 29,881 coverage], [Case 11 with V36A: 0.2% of 27,915 coverage], and [Case 12 with T54S: 99.9% of 33,830 coverage]; Table IV).

Of 10 patients who did not show sustained virological response to triple therapy, telaprevir-resistant variants were detected by direct sequencing during and after treatment in 80.0% (eight patients [Cases 7–14]), and not detected in 20.0% (two patients [Cases 5, 6]). However, telaprevir-resistant variants were detected by ultra-deep sequencing during and after treatment in all 10 patients (Cases 5–14; Table IV).

Evolution of Telaprevir-Resistant Variants Over Time Detected by Ultra-Deep Sequencing

In 3 (Cases 9, 11, 12) of 10 patients who did not show sustained virological response to triple therapy, telaprevir-resistant variants were detected by ultra-deep sequencing at baseline. In Case 9 (relapse), very low frequency variants of V170A (0.4% of 29,881 coverage) at baseline were replaced after treatment by de novo very high frequency variants of A156T (99.6% of 14,757 coverage). In Case 11 (breakthrough), very low frequency variants of V36A (0.2% of 27,915 coverage) at baseline persisted during treatment as very low frequency variants of V36A (0.2% of 5,835 coverage), but de novo high frequency

TABLE III. Profile at Commencement of Triple Therapy, Virological Course, and Efficacy of Treatment

Case	Sex	Age (yrs)	BMI (kg/m^2)	*IL28B*	Core aa70	NS5A ISDR	Previous response	RNA (log IU/ml) Baseline	12 weeks	24 weeks	48 weeks	Efficacy
1	M	50	22.6	TG/CT	Arg70	Wild	Partial	6.6	Negative	Negative	Negative	SVR
2	F	52	25.3	TG/CT	Arg70	Wild	Partial	7.3	Negative	Negative	Negative	SVR
3	M	63	25.5	TG/CT	Arg70	Wild	Partial	7.0	Negative	Negative	Negative	SVR
4	M	50	18.1	TT/CC	Arg70	Wild	Partial	6.6	Negative	Negative	Negative	SVR
5	F	61	26.5	GG/TT	Arg70	Wild	Null	7.1	Negative	Negative	6.9	Relapse
6	M	56	23.6	TG/CT	Gln70	Wild	Partial	6.6	Negative	Negative	6.0	Relapse
7	M	48	24.9	TG/CT	Gln70	Wild	Partial	6.7	Negative	Negative	6.1	Relapse
8	M	40	23.3	TG/CT	Gln70	Wild	Partial	6.4	Negative	Negative	6.8	Relapse
9[a]	F	65	22.7	GG/TT	Gln70	Wild	Null	5.8	Negative[b]	—	6.6[c]	Relapse
10	F	59	22.7	TG/CT	Arg70	Wild	Partial	6.3	3.9	4.3	6.0	Breakthrough
11	M	47	23.7	TG/CT	Gln70	Wild	Null	7.2	Negative	3.8	7.6	Breakthrough
12	F	60	20.9	TG/CT	Gln70	Non-Wild	Null	6.4	Negative	2.1	6.0	Breakthrough
13	F	63	20.4	TG/CT	Gln70	Wild	Null	6.8	2.7	5.9	7.2	Breakthrough
14	F	55	21.0	TG/CT	Gln70	Wild	Null	7.4	4.2	6.9	7.6	Non-response

IL28B, rs8099917/rs12979860 genotypes; SVR, sustained virological response.
[a]Case 9 stopped the triple therapy at 9 weeks due to a fall in Hb concentration.
[b]At 9 weeks.
[c]HCV RNA at 24 weeks after stopping treatment.

TABLE IV. Detection of Telaprevir-Resistant Variants by Direct and Ultra-Deep Sequencing, at Two Time Points (Baseline and Re-Elevation of Viral Load)

		At point of baseline				At point of re-elevation of viral loads				
Case	Position	Direct	Deep	Coverage	Viral loads	Direct	Deep	Coverage	Viral loads	Efficacy
1	aa36	—	—	31,204	6.6	ND	ND	ND	ND	SVR
	aa54	—	—	33,284		ND	ND	ND		
	aa155	—	—	19,468		ND	ND	ND		
	aa156	—	—	22,657		ND	ND	ND		
	aa170	—	—	20,762		ND	ND	ND		
2	aa36	—	—	44,203	7.4	ND	ND	ND	ND	SVR
	aa54	—	—	66,117		ND	ND	ND		
	aa155	—	—	48,863		ND	ND	ND		
	aa156	—	—	55,519		ND	ND	ND		
	aa170	—	—	60,022		ND	ND	ND		
3	aa36	—	—	43,620	7.0	ND	ND	ND	ND	SVR
	aa54	—	—	58,753		ND	ND	ND		
	aa155	—	—	33,249		ND	ND	ND		
	aa156	—	—	36,227		ND	ND	ND		
	aa170	—	—	33,005		ND	ND	ND		
4	aa36	—	—	60,773	6.6	ND	ND	ND	ND	SVR
	aa54	—	—	68,541		ND	ND	ND		
	aa155	—	—	46,512		ND	ND	ND		
	aa156	—	—	48,389		ND	ND	ND		
	aa170	—	—	62,197		ND	ND	ND		
5	aa36	—	—	47,769	7.1	—	—	34,279	5.8	Relapse
	aa54	—	—	66,508		—	—	31,842		
	aa155	—	—	23,751		—	Q (0.2%)	11,572		
	aa156	—	—	25,317		—	T (0.2%)	16,040		
	aa170	—	—	30,807		—	—	10,637		
6	aa36	—	—	70,158	6.6	—	—	49,523	6.0	Relapse
	aa54	—	—	78,419		—	—	73,216		
	aa155	—	—	15,606		—	—	35,998		
	aa156	—	—	15,175		—	T (1.4%)	56,171		
	aa170	—	—	15,218		—	—	52,691		
7	aa36	—	—	40,035	6.7	A	A (81.6%)	16,952	4.5	Relapse
	aa54	—	—	52,685		—	A (0.2%)	30,353		
	aa155	—	—	19,171		—	Q (1.8%)	17,847		
	aa156	—	—	21,407		—	T (0.7%)	19,988		
	aa170	—	—	26,457		—	—	17,339		
8	aa36	—	—	63,035	6.4	—	—	29,802	5.4	Relapse
	aa54	—	—	54,526		A	A (98.2%) · S (0.9%)	23,781		
	aa155	—	—	60,030		—	K (0.3%)	26,846		
	aa156	—	—	59,571		—	—	30,403		
	aa170	—	—	44,816		—	—	24,467		
9	aa36	—	—	32,598	5.8	—	—	8,968	5.4	Relapse
	aa54	—	—	29,903		—	—	14,013		
	aa155	—	—	22,440		—	—	14,499		
	aa156	—	—	26,318		T	T (99.6%)	14,757		
	aa170	—	A (0.4%)	29,881		—	—	17,139		
10	aa36	—	—	299,668	6.3	M	M (94.6%)	51,403	3.9	Breakthrough
	aa54	—	—	370,253		—	S (0.2%)	42,176		
	aa155	—	—	123,791		—	—	9,581		
	aa156	—	—	126,538		—	S (0.7%)	13,028		
	aa170	—	—	116,279		—	—	5,033		
11	aa36	—	A (0.2%)	27,915	7.2	—	A (0.2%)	5,853	3.8	Breakthrough
	aa54	—	—	31,822		A	A (27.7%)	5,032		
	aa155	—	—	8,016		—	Q (0.4%)	9,873		
	aa156	—	—	8,134		—	T (0.3%)	17,178		
	aa170	—	—	19,360		—	—	27,246		
12	aa36	—	—	30,743	6.4	—	C (5.4%) · A (0.2%)	16,095	5.8	Breakthrough
	aa54	S	S (99.9%)	33,830		S	S (99.7%)	26,348		
	aa155	—	—	14,931		K	K (96.1%) · Q (0.4%)	20,630		
	aa156	—	—	15,930		—	—	22,087		
	aa170	—	—	38,447		—	—	24,204		
13	aa36	—	—	75,460	6.8	—	C (0.4%)	36,193	2.7	Breakthrough
	aa54	—	—	80,066		—	S (0.9%) · A (0.2%)	41,127		
	aa155	—	—	18,658		—	—	29,921		
	aa156	—	—	17,175		S	S (99.2%)	29,582		

(*Continued*)

TABLE IV. (*Continued*)

Case	Position	At point of baseline			Viral loads	At point of re-elevation of viral loads			Viral loads	Efficacy
		Direct	Deep	Coverage		Direct	Deep	Coverage		
	aa170	—	—	82,725		—	—	48,491		
14	aa36	—	—	131,802	7.4	—	—	9,803	3.0	Non-response
	aa54	—	—	163,800		S	S (79.4%)	17,273		
	aa155	—	—	65,310		—	—	19,885		
	aa156	—	—	64,594		S	S (99.8%)	20,207		
	aa170	—	—	121,327		—	—	31,243		

Substituted amino acids are shown by standard single-letter codes, and frequencies among the total coverage by ultra-deep sequencing are also presented. Dashes indicate amino acids, except for telaprevir-resistant variants included V36A/C/M/L/G, T54A/S, R155K/T/I/M/G/L/S/Q, A156V/T/S/I/G, V170A. Viral loads (log IU/ml) at two points of baseline or re-elevation are shown.
ND, not done; Direct, direct sequencing; deep, ultra-deep sequencing.

variants of T54A (27.7% of 5,032 coverage) emerged during treatment. In Case 12 (breakthrough), very high frequency variants of T54S (99.9% of 33,830 coverage) at baseline persisted during treatment as very high frequency variants of T54S (99.7% of 26,348 coverage), and de novo very high frequency variants of R155K (96.1% of 20,630 coverage) also emerged during treatment (Table IV).

In 7 (Cases 5, 6, 7, 8, 10, 13, 14) of 10 patients, who did not show sustained virological response to triple therapy, telaprevir-resistant variants were not detected at baseline by ultra-deep sequencing, but de novo resistant variants were detected according to treatment (three patients with V36A/C/M [Cases 7, 10, 13], five with T54A/S [Cases 7, 8, 10, 13, 14], three with R155K/Q [Cases 5, 7, 8], and six with A156S/T [Cases 5, 6, 7, 10, 13, 14]; Table IV).

Thus, the present study using ultra-deep sequencing indicates the emergence of de novo telaprevir-resistant variants regardless of variants frequencies at baseline, and that the emergence of variants after the start of treatment could not be predicted at baseline.

DISCUSSION

Employing ultra-deep sequencing, the present study indicated that de novo telaprevir-resistant variants emerged regardless of variants frequencies at baseline, and that the emergence of variants after the start of triple therapy could not be predicted at baseline. Hence, non-responders to previous therapy (those who failed to achieve sustained virological response to triple therapy) need to be identified to avoid the emergence of telaprevir-resistant variants. Host genetic factors (e.g., *IL28B* genotype), and viral factors (e.g., amino acid substitutions in the core/NS5A region) have often been used as pretreatment predictors of poor virological response to PEG-IFN/ribavirin dual therapy [Akuta et al., 2005; Donlin et al., 2007; El-Shamy et al., 2008; Ge et al., 2009; Suppiah et al., 2009; Tanaka et al., 2009; Maekawa et al., 2012], and telaprevir/PEG-IFN/ribavirin triple therapy [Akuta et al., 2010; Chayama et al., 2011]. However, it is not clear at this stage whether these factors can be used to predict the virological response to triple therapy in non-responders to previous therapy. The present study identified that the T12PR24 regimen could achieve a higher sustained virological response rate in non-responders to previous therapy with the combination of Arg70 and partial response, and suggests that this group of non-responders should especially be selected for triple therapy to overcome problem of telaprevir-resistant variants.

Three previous studies of patients naïve to direct-acting antiviral agents detected telaprevir-resistant variant rates of 13.4% [Shindo et al., 2011], 4.9% [Suzuki et al., 2012], and 9.2% [Vicenti et al., 2012] at baseline using direct sequencing. In the present study, the telaprevir-resistant variant rate detected at baseline by direct sequencing was 7.1%, which is similar to that reported in the above three studies. A recent study using ultra-deep sequencing of patients naïve to direct-acting antiviral agents, showed that rates of telaprevir-resistant variants at baseline were 44.4, 74.1, 18.5, and 25.9% per position for aa36, aa54, aa155, and aa156, respectively [Nasu et al., 2011]. However, in the present study, the rates of resistant variants at baseline using the same technology were 7.1%, 7.1%, 0%, 0%, and 7.1% per position for aa36, aa54, aa155, aa156, and aa170, respectively (Table IV). The following differences could probably explain the differences in the rates between the two studies: (1) Ultra-deep sequencing was performed using the Ion PGM Sequencer (Life Technologies) in the present study, compared with the Illumina Genome Analyzer II (Illumina, San Diego, CA) in the previous study and (2) The previous study was performed in treatment-naïve patients, while the present study was conducted in non-responders to previous PEG-IFN/ribavirin therapy. Further studies of larger number of patients matched for deep sequence platform and clinical background, including past history of treatment, are required to investigate the true frequency of telaprevir-resistant variants.

Interestingly, ultra-deep sequencing identified telaprevir-resistant variants at baseline in two patients (Case 9 with V170A [0.4%], and Case 11 with V36A [0.2%])at very low frequency, but the frequency of resistant variants did not increase over time. This

finding may be due to one or more reasons. One reason is probably related to the high susceptibility of telaprevir-resistant variants to IFN [Hiraga et al., 2011]. Furthermore, this finding probably suggests that a small number of mutant type viral RNA may be incomplete or defective, since a large proportion of viral genomes are thought to be defective due to the high replication and mutation rates of the virus [Bartenschlager and Lohmann, 2000]. Further studies should be performed in order to interpret the significance of the presence of low frequency variants detected by ultra-deep sequencing.

A recent study using the human hepatocyte chimeric mouse model and deep sequencing reported that the rapid emergence of de novo telaprevir-resistant HCV quasispecies was induced by mutation of the wild type strain of HCV in vivo [Hiraga et al., 2011]. In the present study, ultra-deep sequencing did not detect any telaprevir-resistant variants at baseline in seven patients, although de novo resistant variants emerged in all seven patients over time. The present clinical results provide evidence in support of de novo emergence of telaprevir resistance induced by viral mutation.

Recent studies described the use of deep sequencing in detecting resistant variants induced by NS3 protease inhibitors, except for telaprevir. One study applied deep sequencing analysis of HCV-1 in patients treated with protease inhibitor GS-9256/GS-9451 [Svarovskaia et al., 2012]. The results suggested limited viral load suppression with protease inhibitor monotherapy, which failed to suppress preexisting resistant variants, highlighting the need for combination therapy. Another report described the efficacy of re-treatment with protease inhibitor TMC435 as combination therapy in six patients infected with HCV-1, after a full-course of TMC435 monotherapy. Direct sequencing before re-treatment did not detect TMC435-resistant variants, but deep sequencing indicated persistence of low-level of resistant variants in two patients, which could have affected their response to re-treatment [Lenz et al., 2012].

One limitation of the present study is that the existence of very low frequency telaprevir-resistant variants was not investigated long after the cessation of therapy, by ultra-deep sequencing. Further large-scale studies using ultra-deep sequencing should be performed to investigate the effects of telaprevir-resistant variants on the response to treatment using new drugs, including direct-acting antiviral agents.

In conclusion, the present study could not predict the emergence of telaprevir-resistant variants after the start of triple therapy in non-responders to previous therapy, even by using ultra-deep sequencing at baseline. Further large-scale prospective studies are needed to investigate the clinical utility of the ultra-deep sequencing technology in detecting low frequency telaprevir-resistant variants, and to help in the design of more effective therapeutic regimens.

REFERENCES

Akuta N, Suzuki F, Sezaki H, Suzuki Y, Hosaka T, Someya T, Kobayashi M, Saitoh S, Watahiki S, Sato J, Matsuda M, Kobayashi M, Arase Y, Ikeda K, Kumada H. 2005. Association of amino acid substitution pattern in core protein of hepatitis C virus genotype1b high viral load and non-virological response to interferon-ribavirin combination therapy. Intervirology 48:372–380.

Akuta N, Suzuki F, Kawamura Y, Yatsuji H, Sezaki H, Suzuki Y, Hosaka T, Kobayashi M, Kobayashi M, Arase Y, Ikeda K, Kumada H. 2007. Amino acid substitutions in the hepatitis C virus core region are the important predictor of hepatocarcinogenesis. Hepatology 46:1357–1364.

Akuta N, Suzuki F, Hirakawa M, Kawamura Y, Yatsuji H, Sezaki H, Suzuki Y, Hosaka T, Kobayashi M, Kobayashi M, Saitoh S, Arase Y, Ikeda K, Chayama K, Nakamura Y, Kumada H. 2010. Amino acid substitution in hepatitis C virus core region and genetic variation near the interleukin 28B gene predict viral response to telaprevir with peginterferon and ribavirin. Hepatology 52:421–429.

Akuta N, Suzuki F, Seko Y, Kawamura Y, Sezaki H, Suzuki Y, Hosaka T, Kobayashi M, Kobayashi M, Saitoh S, Arase Y, Ikeda K, Kumada H. 2012a. Determinants of response to triple therapy of telaprevir, peginterferon, and ribavirin in previous non-responders infected with HCV genotype 1. J Med Virol 84:1097–1105.

Akuta N, Suzuki F, Seko Y, Kawamura Y, Sezaki H, Suzuki Y, Hosaka T, Kobayashi M, Hara T, Kobayashi M, Saitoh S, Arase Y, Ikeda K, Kumada H. 2012b. Complicated relationships of amino acid substitution in HCV core region and *IL28B* genotype influencing hepatocarcinogenesis. Hepatology 56:2134–2141.

Barbotte L, Ahmed-Belkacem A, Chevaliez S, Soulier A, Hézode C, Wajcman H, Bartels DJ, Zhou Y, Ardzinski A, Mani N, Rao BG, George S, Kwong A, Pawlotsky JM. 2010. Characterization of V36C, a novel amino acid substitution conferring hepatitis C virus (HCV) resistance to telaprevir, a potent peptidomimetic inhibitor of HCV protease. Antimicrob Agents Chemother 54: 2681–2683.

Bartenschlager R, Lohmann V. 2000. Replication of hepatitis C virus. J Gen Virol 81:1631–1648.

Bull RA, Luciani F, McElroy K, Gaudieri S, Pham ST, Chopra A, Cameron B, Maher L, Dore GJ, White PA, Lloyd AR. 2011. Sequential bottlenecks drive viral evolution in early acute hepatitis C virus infection. PLoS Pathog 7:e1002243.

Chayama K, Hayes CN, Abe H, Miki D, Ochi H, Karino Y, Toyota J, Nakamura Y, Kamatani N, Sezaki H, Kobayashi M, Akuta N, Suzuki F, Kumada H. 2011. *IL28B* but not *ITPA* polymorphism is predictive of response to pegylated interferon, ribavirin, and telaprevir triple therapy in patients with genotype 1 hepatitis C. J Infect Dis 204:84–93.

Donlin MJ, Cannon NA, Yao E, Li J, Wahed A, Taylor MW, Belle SH, Di Bisceglie AM, Aurora R, Tavis JE. 2007. Pretreatment sequence diversity differences in the full-length hepatitis C virus open reading frame correlate with early response to therapy. J Virol 81:8211–8224.

Elliott AM, Radecki J, Moghis B, Li X, Kammesheidt A. 2012. Rapid detection of the ACMG/ACOG-recommended 23 CFTR disease-causing mutations using ion torrent semiconductor sequencing. J Biomol Tech 23:24–30.

El-Shamy A, Nagano-Fujii M, Sasase N, Imoto S, Kim SR, Hotta H. 2008. Sequence variation in hepatitis C virus nonstructural protein 5A predicts clinical outcome of pegylated interferon/ribavirin combination therapy. Hepatology 48:38–47.

Enomoto N, Sakuma I, Asahina Y, Kurosaki M, Murakami T, Yamamoto C, Ogura Y, Izumi N, Marumo F, Sato C. 1996. Mutations in the nonstructural protein 5A gene and response to interferon in patients with chronic hepatitis C virus 1b infection. N Engl J Med 334:77–81.

Ge D, Fellay J, Thompson AJ, Simon JS, Shianna KV, Urban TJ, Heinzen EL, Qiu P, Bertelsen AH, Muir AJ, Sulkowski M, McHutchison JG, Goldstein DB. 2009. Genetic variation in IL28B predicts hepatitis C treatment-induced viral clearance. Nature 461:399–401.

Hézode C, Forestier N, Dusheiko G, Ferenci P, Pol S, Goeser T, Bronowicki JP, Bourlière M, Gharakhanian S, Bengtsson L, McNair L, George S, Kieffer T, Kwong A, Kauffman RS, Alam J,

Pawlotsky JM, Zeuzem S, PROVE2 Study Team. 2009. Telaprevir and peginterferon with or without ribavirin for chronic HCV infection. N Engl J Med 360:1839–1850.

Hiraga N, Imamura M, Abe H, Hayes CN, Kono T, Onishi M, Tsuge M, Takahashi S, Ochi H, Iwao E, Kamiya N, Yamada I, Tateno C, Yoshizato K, Matsui H, Kanai A, Inaba T, Tanaka S, Chayama K. 2011. Rapid emergence of telaprevir resistant hepatitis C virus strain from wildtype clone in vivo. Hepatology 54:781–788.

Kato N, Hijikata M, Ootsuyama Y, Nakagawa M, Ohkoshi S, Sugimura T, Shimotohno K. 1990. Molecular cloning of the human hepatitis C virus genome from Japanese patients with non-A, non-B hepatitis. Proc Natl Acad Sci USA 87:9524–9528.

Kieffer TL, Sarrazin C, Miller JS, Welker MW, Forestier N, Reesink HW, Kwong AD, Zeuzem S. 2007. Telaprevir and pegylated interferon-alpha-2a inhibit wild-type and resistant genotype 1 hepatitis C virus replication in patients. Hepatology 46:631–639.

Kumada H, Toyota J, Okanoue T, Chayama K, Tsubouchi H, Hayashi N. 2012. Telaprevir with peginterferon and ribavirin for treatment-naive patients chronically infected with HCV of genotype 1 in Japan. J Hepatol 56:78–84.

Lenz O, de Bruijne J, Vijgen L, Verbinnen T, Weegink C, Van Marck H, Vandenbroucke I, Peeters M, Simmen K, Fanning G, Verloes R, Picchio G, Reesink H. 2012. Efficacy of re-treatment with TMC435 as combination therapy in hepatitis C virus-infected patients following TMC435 monotherapy. Gastroenterology 143:1176–1178.

Lin C, Gates CA, Rao BG, Brennan DL, Fulghum JR, Luong YP, Frantz JD, Lin K, Ma S, Wei YY, Perni RB, Kwong AD. 2005. In vitro studies of cross-resistance mutations against two hepatitis C virus serine protease inhibitors, VX-950 and BILN 2061. J Biol Chem 280:36784–36791.

Lin C, Kwong AD, Perni RB. 2006. Discovery and development of VX-950, a novel, covalent, and reversible inhibitor of hepatitis C virus NS3. 4A serine protease. Infect Disord Drug Targets 6:3–16.

Maekawa S, Sakamoto M, Miura M, Kadokura M, Sueki R, Komase K, Shindo H, Komatsu N, Shindo K, Kanayama A, Ohmori T, Amemiya F, Takano S, Yamaguchi T, Nakayama Y, Kitamura T, Inoue T, Okada S, Enomoto N. 2012. Comprehensive analysis for viral elements and interleukin-28B polymorphisms in response to pegylated interferon plus ribavirin therapy in hepatitis C virus 1B infection. Hepatology 56:1611–1621.

McHutchison JG, Everson GT, Gordon SC, Jacobson IM, Sulkowski M, Kauffman R, McNair L, Alam J, Muir AJ, PROVE1 Study Team. 2009. Telaprevir with peginterferon and ribavirin for chronic HCV genotype 1 infection. N Engl J Med 360:1827–1838.

McHutchison JG, Manns MP, Muir AJ, Terrault NA, Jacobson IM, Afdhal NH, Heathcote EJ, Zeuzem S, Reesink HW, Garg J, Bsharat M, George S, Kauffman RS, Adda N, Di Bisceglie AM, PROVE3 Study Team. 2010. Telaprevir for previously treated chronic HCV infection. N Engl J Med 362:1292–1303.

Nasu A, Marusawa H, Ueda Y, Nishijima N, Takahashi K, Osaki Y, Yamashita Y, Inokuma T, Tamada T, Fujiwara T, Sato F, Shimizu K, Chiba T. 2011. Genetic heterogeneity of hepatitis C virus in association with antiviral therapy determined by ultra-deep sequencing. PLoS ONE 6:e24907.

Ninomiya M, Ueno Y, Funayama R, Nagashima T, Nishida Y, Kondo Y, Inoue J, Kakazu E, Kimura O, Nakayama K, Shimosegawa T. 2012. Use of illumina deep sequencing technology to differentiate hepatitis C virus variants. J Clin Microbiol 50:857–866.

Ohnishi Y, Tanaka T, Ozaki K, Yamada R, Suzuki H, Nakamura Y. 2001. A high-throughput SNP typing system for genome-wide association studies. J Hum Genet 46:471–477.

Romano KP, Ali A, Royer WE, Schiffer CA. 2010. Drug resistance against HCV NS3/4A inhibitors is defined by the balance of substrate recognition versus inhibitor binding. Proc Natl Acad Sci USA 107:20986–20991.

Shindo H, Maekawa S, Komase K, Sueki R, Miura M, Kadokura M, Shindo K, Amemiya F, Kitamura T, Nakayama Y, Inoue T, Sakamoto M, Okada SI, Asahina Y, Izumi N, Honda M, Kaneko S, Enomoto N. Characterization of naturally occurring protease inhibitor-resistance mutations in genotype 1b hepatitis C virus patients. Hepatol Int 2011. [Epub ahead of print].

Suppiah V, Moldovan M, Ahlenstiel G, Berg T, Weltman M, Abate ML, Bassendine M, Spengler U, Dore GJ, Powell E, Riordan S, Sheridan D, Smedile A, Fragomeli V, Müller T, Bahlo M, Stewart GJ, Booth DR, George J. 2009. *IL28B* is associated with response to chronic hepatitis C interferon-alpha and ribavirin therapy. Nat Genet 41:1100–1104.

Suzuki A, Yamada R, Chang X, Tokuhiro S, Sawada T, Suzuki M, Nagasaki M, Nakayama-Hamada M, Kawaida R, Ono M, Ohtsuki M, Furukawa H, Yoshino S, Yukioka M, Tohma S, Matsubara T, Wakitani S, Teshima R, Nishioka Y, Sekine A, Iida A, Takahashi A, Tsunoda T, Nakamura Y, Yamamoto K. 2003. Functional haplotypes of PADI4, encoding citrullinating enzyme peptidylarginie deminase 4, are associated with rheumatoid arthritis. Nat Genet 34:395–402.

Suzuki F, Sezaki H, Akuta N, Suzuki Y, Seko Y, Kawamura Y, Hosaka T, Kobayashi M, Saito S, Arase Y, Ikeda K, Kobayashi M, Mineta R, Watahiki S, Miyakawa Y, Kumada H. 2012. Prevalence of hepatitis C virus variants resistant to NS3 protease inhibitors or the NS5A inhibitor (BMS-790052) in hepatitis patients with genotype 1b. J Clin Virol 54:352–354.

Svarovskaia ES, Martin R, McHutchison JG, Miller MD, Mo H. 2012. Abundant drug-resistant NS3 mutants detected by deep sequencing in hepatitis C virus-infected patients undergoing NS3 protease inhibitor monotherapy. J Clin Microbiol 50:3267–3274.

Tanaka Y, Nishida N, Sugiyama M, Kurosaki M, Matsuura K, Sakamoto N, Nakagawa M, Korenaga M, Hino K, Hige S, Ito Y, Mita E, Tanaka E, Mochida S, Murawaki Y, Honda M, Sakai A, Hiasa Y, Nishiguchi S, Koike A, Sakaida I, Imamura M, Ito K, Yano K, Masaki N, Sugauchi F, Izumi N, Tokunaga K, Mizokami M. 2009. Genome-wide association of IL28B with response to pegylated interferon-alpha and ribavirin therapy for chronic hepatitis C. Nat Genet 41:1105–1109.

Vicenti I, Rosi A, Saladini F, Meini G, Pippi F, Rossetti B, Sidella L, Di Giambenedetto S, Almi P, De Luca A, Caudai C, Zazzi M. 2012. Naturally occurring hepatitis C virus (HCV) NS3/4A protease inhibitor resistance-related mutations in HCV genotype 1-infected subjects in Italy. J Antimicrob Chemother 67:984–987.

Vogel U, Szczepanowski R, Claus H, Jünemann S, Prior K, Harmsen D. 2012. Ion torrent personal genome machine sequencing for genomic typing of Neisseria meningitidis for rapid determination of multiple layers of typing information. J Clin Microbiol 50:1889–1894.

Hepatol Int (2013) 7:850–858
DOI 10.1007/s12072-012-9419-7

Three-dimensional magnetic resonance imaging for stringent diagnosis of advanced fibrosis associated with nonalcoholic steatohepatitis

Yusuke Kawamura · Satoshi Saitoh · Yasuji Arase · Kenji Ikeda · Taito Fukushima · Tasuku Hara · Yuya Seko · Tetsuya Hosaka · Masahiro Kobayashi · Hitomi Sezaki · Norio Akuta · Fumitaka Suzuki · Yoshiyuki Suzuki · Kei Fukuzawa · Yusuke Hamada · Junji Takahashi · Mariko Kobayashi · Hiromitsu Kumada

Received: 19 September 2012 / Accepted: 8 December 2012 / Published online: 30 January 2013

Abstract
Background The definitive diagnosis of nonalcoholic steatohepatitis (NASH) is currently based on histopathological assessment. This study aimed to elucidate the utility of a novel noninvasive method, three-dimensional magnetic resonance imaging (3D-MRI), for diagnosing advanced fibrosis in patients with NASH, using histopathological diagnosis as the reference standard.
Methods This retrospective study included 30 consecutive patients who had been diagnosed with NASH by histopathology and had undergone 3D-MRI before biopsy. 3D-MRI provided a three-dimensional reconstruction of the liver from contrast-enhanced hepatobiliary phase MR images. In the present study, histopathological advanced fibrosis was defined as stage 3 and 4 NASH. Advanced fibrosis, diagnosed by 3D-MRI, was considered to be diffuse irregularity of the entire surface of the liver. The diagnostic features of 3D-MRI and the noninvasive evaluation systems (APRI, FIB-4 index, and BARD score) for identifying advanced and nonadvanced fibrosis of NASH were determined and compared.
Results Nine (30 %) of the 30 study patients were diagnosed histopathologically with advanced fibrosis, and 11 (37 %) of 30 patients were diagnosed with advanced fibrosis using 3D-MRI. The sensitivity, specificity, positive predictive value (PPV), and negative predictive value (NPV) of 3D-MRI for diagnosing advanced fibrosis were 100, 90, 82, and 100 %, respectively. The sensitivities of APRI, the FIB-4 index, and BARD score ranged from 78 to 89 %, the specificities from 71 to 90 %, the PPVs from 54 to 78 %, and the NPVs from 88 to 94 %.
Conclusion Compared with the common noninvasive methods for diagnosing advanced fibrosis associated with NASH, 3D-MRI was more accurate.

Keywords Nonalcoholic fatty liver disease · Nonalcoholic steatohepatitis · Advanced fibrosis · 3D-MRI · Virtual MR-laparoscopy

Y. Kawamura (✉) · S. Saitoh · Y. Arase · K. Ikeda · T. Fukushima · T. Hara · Y. Seko · T. Hosaka · M. Kobayashi · H. Sezaki · N. Akuta · F. Suzuki · Y. Suzuki · H. Kumada
Department of Hepatology, Toranomon Hospital, 2-2-2, Toranomon, Minato-ku, Tokyo 105-8470, Japan
e-mail: k-yusuke@toranomon.gr.jp

Y. Kawamura · S. Saitoh · Y. Arase · K. Ikeda · T. Fukushima · T. Hara · Y. Seko · T. Hosaka · M. Kobayashi · H. Sezaki · N. Akuta · F. Suzuki · Y. Suzuki · K. Fukuzawa · Y. Hamada · J. Takahashi · M. Kobayashi · H. Kumada
Okinaka Memorial Institute for Medical Research, Toranomon Hospital, Tokyo, Japan

K. Fukuzawa · Y. Hamada · J. Takahashi
Department of Radiology, Toranomon Hospital, Tokyo, Japan

M. Kobayashi
Research Institute for Hepatology, Toranomon Hospital, Tokyo, Japan

Introduction

Nonalcoholic fatty liver disease (NAFLD) is a common cause of chronic liver disease in Western countries [1–4], and recently it has become common in many Asian nations [5, 6]. In particular, patients with nonalcoholic steatohepatitis (NASH), a subcategory of NAFLD, are at an increased risk for developing hepatocellular carcinoma [7]. Like patients with viral hepatitis, NAFLD patients with advanced fibrosis have an increased risk of developing hepatocellular carcinoma [8–10]. Currently, NASH can be diagnosed only by histopathology. Usually, chronic liver

disease is definitively diagnosed using either histopathological examination of a biopsy specimen or visualization of the surface of the liver at laparoscopy. Kelling [11] revolutionized investigations of liver disease when he first described laparoscopy in 1923. Laparoscopy-guided liver biopsy is considered by many to be the most accurate method of diagnosing liver disease, especially liver cirrhosis [12, 13]. However, the use of laparoscopy for the diagnosis of liver disease has decreased over the past decade, because there are misconceptions about the overall safety and rate of complications. Laparoscopy is generally a more complex procedure than ultrasonography (US)-guided biopsy.

The number of patients with NAFLD is expected to increase. In actuality, US alone is being used to identify many patients with NAFLD to avoid invasive histological diagnoses. Therefore, because of increased cost, possible risks (risk of bleeding, allergic reaction caused by local anesthetics, and advanced age), and health-care resource usage, invasive liver biopsy is poorly suited as a diagnostic method for such a prevalent condition. Furthermore, the NASH lesions are unevenly distributed throughout the liver parenchyma; therefore, liver biopsy has inherent sampling errors, which can lead to substantial inaccuracies in stratification and staging [14].

Because of the problems with biopsy for evaluating patients with liver disease, noninvasive diagnostic tools that are not based on image analysis and are easy to implement for outpatient medical care have been used. These include the following: the aspartate aminotransferase (AST) to platelet ratio index (APRI) [15], FIB-4 index [16], and BARD score [which includes the following three variables: body mass index (BMI), AST/alanine aminotransferase (ALT) ratio, and diabetes] [17]. The APRI was developed for the prediction of significant fibrosis in patients with chronic hepatitis C [15], and its utility for patients with NAFLD has also been reported [18]. The FIB-4 index was developed as a noninvasive panel for staging liver disease in patients with human immunodeficiency virus/hepatitis C virus (HCV) coinfection [16]. It is based on patient age and values for AST, ALT, and platelet count, which are routinely measured and thus available for virtually all patients with liver disease. This index has also been independently validated in subjects with HCV infection alone [19]. It was recently demonstrated that its performance characteristics for the diagnosis of advanced fibrosis in NAFLD are better than those of other similar noninvasive diagnostic panels [20].

More recently, the BARD score, a noninvasive system for predicting advanced fibrosis in patients with NALFD, was introduced [17]. In addition, the usefulness of other noninvasive strategies for predicting fibrosis in patients with NAFLD has been reported, including transient sonoelastography [21, 22], acoustic radiation force impulse imaging (ARFI) [23], and magnetic resonance (MR) elastography [24]. And finally, a new contrast medium for MR imaging, gadolinium-ethoxybenzyl-diethylenetriamine penta-acetic acid (Gd-EOB-DTPA), has been introduced. Gd-EOB-DTPA is a bimodal, intracellular, liver-specific contrast agent, which has been postulated to be superior for the detection and characterization of liver lesions compared with nonspecific extracellular contrast agents [25–29]. Because Gd-EOB-DTPA is taken up selectively by hepatocytes, we were able to acquire higher contrast parenchymal images of the liver during the hepatobiliary phase than could be obtained with other contrast agents. We were then able to reconstruct virtual 3D images from the enhanced MR imaging data. We have called this procedure "virtual MR-laparoscopy" for 3D imaging of the liver, or 3D-MRI. The primary role of liver biopsy in the evaluation of patients with NAFLD is the exclusion of advanced fibrosis and/or cirrhosis, because these conditions affect and alter the clinical management and follow-up of these patients. Therefore, in the present study, we aimed to elucidate the utility of noninvasive 3D-MRI for diagnosing advanced fibrosis in patients with NAFLD, and we compared its diagnostic characteristics with other noninvasive predictive strategies (APRI, FIB-4 index, and BARD score).

Patients and methods

Study population

From January 2011 to July 2012, 129 patients were diagnosed with NASH based on histopathological evaluation at Toranomon Hospital, Tokyo, Japan. Thirty of these patients were enrolled in this retrospective study. The criteria for participation included the following: (1) undergoing 3D-MRI within 1 year before histological examination, (2) past daily alcohol intake of <20 g/day, (3) negative for serum hepatitis C virus antibodies, hepatitis B surface antigen, antinuclear antibodies, and antimitochondrial antibodies, as determined by radioimmunoassay, enzyme-linked immunosorbent assay, or spot hybridization, (4) no underlying systemic autoimmune diseases, such as systemic lupus erythematosus and rheumatoid arthritis, and (5) no underlying metabolic diseases, such as hemochromatosis, alpha-1-antitrypsin deficiency, and Wilson disease.

All patients underwent whole-liver MR image screening for early hepatocellular carcinoma and to assess the extent of liver disease.

The study was approved by the Institutional Review Board of our hospital.

Histopathological examination of the liver

Liver biopsy specimens were obtained using a 14-gauge modified Vim-Silverman needle (Tohoku University Style, Kakinuma Factory, Tokyo, Japan), 16-gauge core tissue biopsy needle (Bard Peripheral Vascular Inc.; Tempe, AZ, USA), or surgical resection. Specimens were fixed in 10 % formalin, and the sections were stained with hematoxylin-eosin, Masson trichrome, silver impregnation, and periodic acid-Schiff after diastase digestion. Fibrosis was scored using the five-grade scale proposed by Brunt et al. [30] as follows: stage 0, normal connective tissue; stage 1, zone 3 (pericentral vein area) perisinusoidal/pericellular fibrosis; stage 2, zone 3 perisinusoidal/pericellular fibrosis with focal or extensive periportal fibrosis; stage 3, bridging or septal fibrosis; and stage 4, cirrhosis.

In the present study, we defined histologically advanced fibrosis as stage 3 and 4 NASH.

Twenty (67 %) of 30 patients underwent US-guided biopsy using a 16-gauge core tissue biopsy needle, 9 (30 %) of 30 underwent laparoscopy-guided biopsy using a 14-gauge modified Vim-Silverman needle, and 1 (3 %) of 30 underwent surgical resection for hepatocellular carcinoma that had been found on 3D-MRI. The resected specimen consisted of the tumor plus tumor-free tissue.

Calculation of APRI and prediction of advanced fibrosis

The APRI was calculated according to the following formula:

$$\text{APRI} = \frac{\text{AST level}(/\text{ULN}*)}{\text{Platelet count } (10^9/\text{L})} \times 100$$

*ULN, AST upper level of normal (33 IU/l).

As previously reported, an APRI >1.50 is predictive of advanced fibrosis [positive predictive value (PPV), 88 %; negative predictive value (NPV), 64 %] [15]. In association with the APRI, hepatic fibrosis was assessed using the Ishak fibrosis scoring system [31]. Advanced fibrosis was defined as an Ishak score of ≥3 (presence of occasional bridging fibrosis). However, another investigator recently concluded that for patients with NAFLD or NASH, an APRI >0.98 was more suitable for predicting advanced fibrosis (NASH stage 3 and 4) (sensitivity 75 %, specificity 86 %, PPV 54 %, NPV 93 %) [18].

Calculation of FIB-4 index and prediction of advanced fibrosis

The FIB-4 index was calculated according to the following formula:

$$\text{FIB4} - \text{index} = \frac{\text{Age(year)} \times \text{AST level}}{\text{Platelet count } (10^9/\text{L}) \times \text{ALT level}^{1/2}}$$

As previously reported, a FIB-4 index >3.25 is predictive of advanced fibrosis (PPV 65 %, NPV 83 %) [16]. However, Shah et al. [20] reported that a FIB-4 index >2.67 was predictive of advanced fibrosis in NAFLD patients (PPV 80 %, NPV 83 %).

In association with the FIB-4 index, hepatic fibrosis was assessed using the Ishak fibrosis scoring system [31]. Advanced fibrosis was defined as an Ishak score of ≥4 (presence of marked bridging fibrosis) [16].

Calculation of BARD score and prediction of advanced fibrosis

The following points were assigned to each variable making up the BARD scoring system: BMI ≥28 kg/m^2, 1 point, AST/ALT ratio ≥0.8, 2 points; presence of diabetes, 1 point. Thus, the scores range from 0 to 4. As previously reported, BARD scores of 2–4 are associated with an odds ratio for advanced fibrosis of 17 (PPV 43 %, NPV 96 %) [17]. A patient with a BARD score ranging from 2 to 4 plus NASH stage 3 or 4 was considered to have advanced fibrosis.

Image acquisition: 3D-MRI

All patients underwent MRI at 1.5 T (Avanto; Siemens-Asahi Meditec, Tokyo, Japan) with a phased-array coil for signal detection. All patients were imaged with the following pulse sequence: transverse 3D of the liver with fat suppression (volumetric interpolated breath-hold examination) in a single breath hold (25 s) at the hepatobiliary phase (20 min after injection of the contrast medium). The contrast medium was Gd-EOB-DTPA (Primovist; Bayer Schering Pharma, Berlin, Germany) at a dose of 0.025 mmol/kg body weight (0.1 ml/kg). The following MRI parameters were used: TR 4.3 ms, TE 2.1 ms, flip angle 15°, parallel imaging factor 2 (GRAPPA), slice thickness 1.5 mm, matrix 192 × 320, and field of view 360 mm. 3D reconstructions of the liver were rendered from enhanced MRI data from the hepatobiliary phase using ZIO STAION (Zaio Software, Tokyo, Japan). The image resolution of each reconstructed figure of the liver provided by 3D-MRI was 512 × 512 pixels.

Various structures around the liver on the 3D image were manually marked and then removed digitally. Finally, the liver was extracted on the workstation. The following findings were noted on 3D-MRI: (1) irregular liver surface, (2) enlargement of the lateral segment, and (3) atrophy of the right lobe. The 3D-MRI findings of the liver surface were classified as follows: (1) smooth (essentially smooth surface of the entire liver or with limited areas of

depression), (2) partially irregular (several interconnected depressions on the surface, mainly in the left lobe of the liver, with rippled or speckled appearance), and (3) diffusely irregular (including diffuse small irregularities or large irregularities with areas of nodularity).

MR image acquisition and 3D reconstruction of the liver were performed by three expert radiologic technologists. The 3D-MR images were evaluated for degree of fibrosis (nonadvanced or advanced fibrosis) by a conference of three expert hepatologists who were blinded to the pathological results. Each hepatologist had 10 or more years of experience performing conventional diagnostic laparoscopy to assess chronic liver disease.

Definition of advanced fibrosis according to APRI, FIB-4 index, BARD score, and 3D-MRI

Advanced fibrosis was defined as follows: (1) APRI >0.98, (2) FIB-4 index >2.67, (3) BARD score = 2–4, and (4) image from 3D-MRI showing diffuse irregularity of the surface of the liver (including diffuse small irregularities or large irregularities with areas of nodularity).

Statistical analysis

Differences in demographic features, laboratory data, and the features of liver biopsy specimens between patients with advanced fibrosis versus patients with nonadvanced fibrosis were analyzed by the Fisher's exact test and Mann-Whitney *U* test. The sensitivity, specificity, PPV, and NPV for identifying advanced and nonadvanced fibrosis were determined for each evaluation system (APRI, FIB-4 index, and BARD score) and 3D-MRI. A p value of <0.05 was considered statistically significant. Data analysis was performed using the Statistical Package for Social Sciences, version 11.0 (SPSS Inc., Chicago, IL, USA).

Results

Clinical and demographic features of patients

Table 1 summarizes the demographic and clinical profiles of the 30 study patients. The patients with advanced

Table 1 Clinical and demographic features of patients with nonalcoholic steatohepatitis who underwent three-dimensional magnetic resonance imaging

	All patients	Nonadvanced fibrosis (stage 1–2) $n = 21$	Advanced fibrosis (stage 3–4) $n = 9$	p value
Gender (M:F)	22:8	17:4	5:4	0.195
Age (years)[a]	59.5 (29–80)	47 (29–73)	63 (51–80)	0.032
Body mass index (kg/m^2)[a]	25.8 (20.8–37.9)	25.4 (20.9–35.1)	26.2 (20.8–37.9)	0.533
Albumin (g/dl)[a]	4.2 (3.6–4.7)	4.2 (3.8–4.7)	3.9 (3.6–4.4)	0.086
Total bilirubin (mg/dl)[a]	0.9 (0.4–1.5)	0.8 (0.4–1.2)	0.9 (0.5–1.5)	0.150
AST (IU/l)[a]	48 (18–198)	41 (18–198)	48 (29–150)	0.422
ALT (IU/l)[a]	76.5 (22–275)	83 (22–275)	45 (22–194)	0.077
γ-GTP (IU/l)[a]	57.5 (15–502)	67 (15–502)	54 (34–125)	0.929
Platelet count (× 10^3/μl)[a]	196 (65–318)	215 (104–318)	181 (65–207)	0.002
Hyaluronic acid (μg/l)	28 (4–196)	21 (4–83)	127 (47–196)	<0.001
Diabetes mellitus (yes/no)	6:24	4:17	2:7	1.000
Uric acid (mg/dl)[a]	6.4 (3.6–9.6)	6.7 (4.7–8.9)	5.3 (3.6–9.6)	0.104
Total cholesterol (mg/dl)[a]	193.5 (94–265)	206 (94–265)	172 (107–223)	0.070
Triglyceride (mg/dl)[a]	144.5 (38–355)	157 (38–276)	140 (40–355)	0.965
LDL-cholesterol (mg/dl)[a]	104.5 (24–177)	113 (24–177)	85 (28–124)	0.025
HDL-cholesterol (mg/dl)[a]	45 (22–76)	45 (28–76)	41 (22–59)	0.304
Needle biopsy specimens of the liver ($n = 29$)[b]				
		$n = 21$	$n = 8$	
Length of specimens (mm)	15 (9–27)	15 (9–27)	20.5 (13–26)	0.024
Number of portal areas	6 (2–21)	5 (2–21)	9.5 (6–12)	0.006

ALT alanine aminotransferase, *AST* aspartate aminotransferase, *γ-GTP* gamma-glutamyl transpeptidase, *HDL* high-density lipoprotein, *LDH* lactate dehydrogenase, *LDL* low-density lipoprotein

[a] Expressed as median (minimum, maximum)

[b] One patient who underwent surgical resection for hepatocellular carcinoma was excluded from quality evaluation of the needle biopsy specimens

fibrosis were significantly older, and they had significantly lower platelet counts, lower low-density lipoprotein-cholesterol levels, and higher hyaluronic acid levels compared with the patients with nonadvanced fibrosis. With regard to the characterization of the needle biopsy specimens (one patient undergoing surgical resection for hepatocellular carcinoma was excluded from quality evaluation of the needle biopsy specimens), the patients with advanced fibrosis had significantly larger specimens and higher numbers of portal areas.

3D-MRI and histological NASH stage

Figure 1a–d shows 3D-MRI figures that corresponded to the different histological NASH stages. These 3D-MRI figures demonstrate that in addition to altered shape of the liver, the irregularities on the surface of the liver gradually extended from the lateral segment to the right lobe. There were nine patients with the Fig. 1a pattern, and all (100 %) were histopathologically diagnosed with NASH stage 1. Of ten patients with the Fig. 1b pattern, five (50 %) were diagnosed with NASH stage 1 and five with NASH stage 2. Of 9 patients with the Fig. 1c pattern, 5 (56 %) were diagnosed with NASH stage 3, 2 (22 %) with NASH stage 4, and 2 with NASH stage 1. Two patients (7 %) had the Fig. 1d pattern, and both were diagnosed with NASH stage 4. Diffuse irregularities of the entire surface of the liver were characteristic of patients with NASH stage 3 and 4; therefore, we designated 3D-MR images showing irregularities of the entire surface of the liver as advanced fibrosis (Fig. 1c, d). A total of 11 (37 %) of 30 patients were diagnosed with advanced fibrosis from the figures obtained by 3D-MRI.

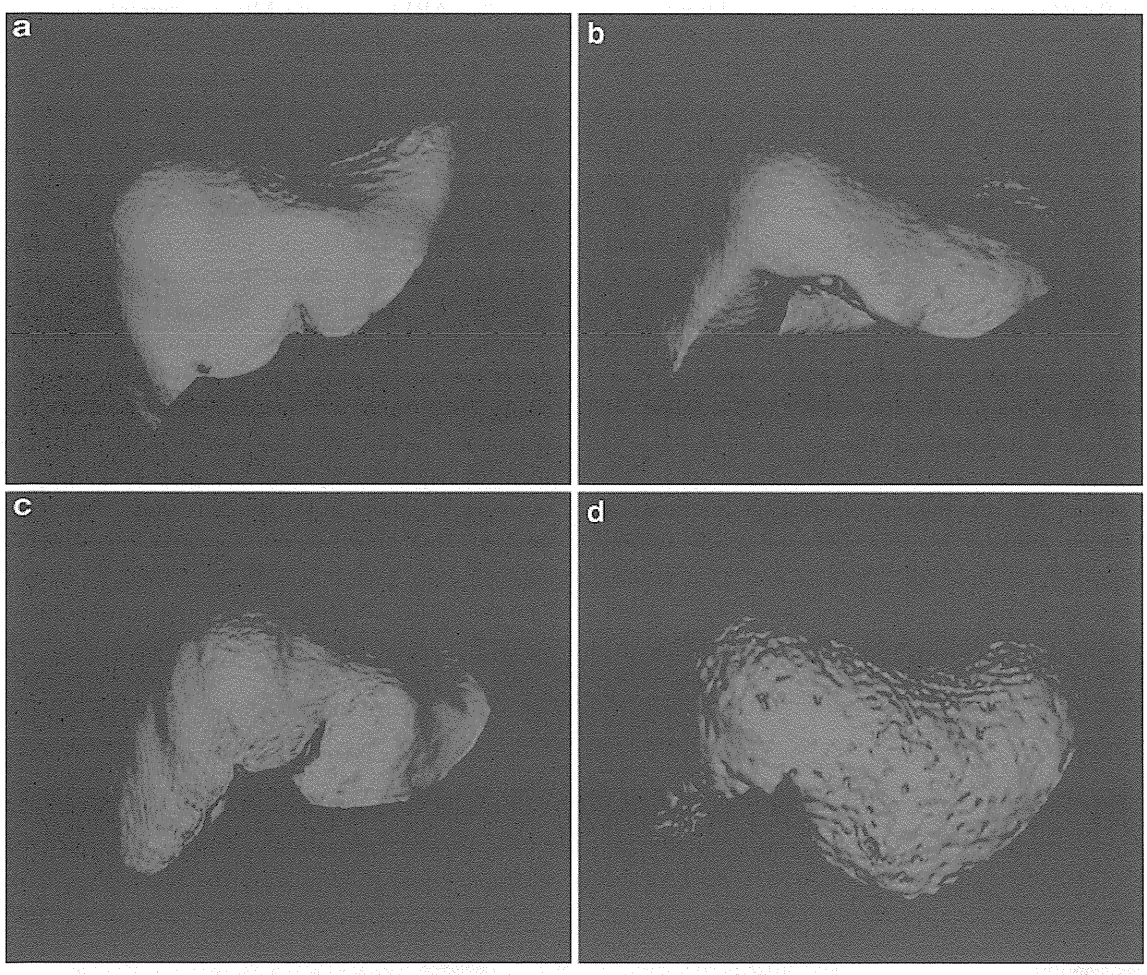

Fig. 1 **a** Three-dimensional magnetic resonance image of nonadvanced liver fibrosis in nonalcoholic steatohepatitis (NASH), stage 1, showing a smooth liver surface and enlarged lateral segment. **b** Image of nonadvanced fibrosis, NASH stage 2, showing localized small irregularities of the surface of the liver and an enlarged lateral segment. **c** Image of advanced fibrosis, NASH stage 3, showing diffuse small irregularities of the surface of the liver and enlarged lateral segment. **d** Image of advanced fibrosis, NASH stage 4, showing diffuse large irregularities of the surface of the liver, an enlarged lateral segment, and atrophic right lobe

Figures 2 and 3 are conventional laparoscopic images of livers of patients with advanced fibrosis (NASH stage 3 and 4, respectively). Figure 2a, b shows diffuse small irregularities of the entire surface of the liver, and the surface of the left lobe (Fig. 2b) has diffuse small irregularities and a large nodular area. The histological diagnosis of this patient was NASH stage 3, and the 3D-MR image of this patient is also shown in Fig. 1c. Figure 3a, b shows diffuse bilobular large irregularities and nodular areas of the surface of the liver. The histological diagnosis of this patient was NASH stage 4, and the 3D-MR image of this patient is also shown in Fig. 1d.

In the present study, one patient was found to have hepatocellular carcinoma on MRI. However, the tumor was small (26 × 22 mm) and occupied a small proportion of the area of the entire surface of the liver; therefore, the diagnostic evaluation was not affected.

Diagnostic features of 3D-MRI and the APRI, FIB-4 index, and BARD scoring systems for advanced fibrosis of the liver

Table 2 summarizes the diagnostic features of 3D-MRI and each scoring system for advanced fibrosis. For the scoring systems (APRI, FIB-4 index, and BARD), the sensitivity ranged from 78 to 89 %, specificity from 71 to 90 %, PPV from 54 to 78 %, and NPV from 88 to 94 %. For 3D-MRI, the sensitivity was 100 %, specificity 90 %, PPV 82 %, and NPV 100 %.

Distributions of patients with advanced fibrosis of the liver according to 3D-MRI, APRI, FIB-4 index, and BARD, and histopathology

Figure 4 shows the distribution of patients predicted to have advanced fibrosis by 3D-MRI and each scoring system, along with the distribution of patients diagnosed with advanced fibrosis by histopathological evaluation. The scoring systems showed more varied distributions compared with 3D-MRI, which showed a uniform distribution that was similar to the histopathological distribution.

Discussion

Up to now, the definitive diagnosis of NASH has been based on histopathological evaluation. However, in Japan, many patients with NAFLD are diagnosed with NASH using US only, because liver biopsies have a risk of major complications such as intraperitoneal bleeding. However, some noninvasive scoring systems (APRI, BARD, and the FIB-4 index) for predicting fibrosis have become available [17]. In addition, the usefulness of other noninvasive strategies for predicting fibrosis in patients with NAFLD has been reported, including transient sonoelastography [21, 22], ARFI [23], and MR elastography [24]. However, these diagnostic methods may lack sensitivity for identifying advanced fibrosis. In addition, for the majority of patients with NAFLD, these methods of prediction usually have weak objectivity and persuasive power. Therefore, a more accurate noninvasive evaluation method is needed. In the present study, we described and reported on the use of "virtual MR-laparoscopy" for 3D imaging of the liver, or 3D-MRI. Although 3D-MRI has qualitative and subjective features, we found that it accurately predicted advanced fibrosis, because it could easily provide visualization of the entire surface of the liver, and evaluation was comparatively easy for physicians experienced with conventional diagnostic laparoscopy for chronic liver disease or treatment of hepatobiliary diseases such as cholecystolithiasis or hepatic tumor. In the present study, 3D-MRI demonstrated a high positive and negative predictive value for

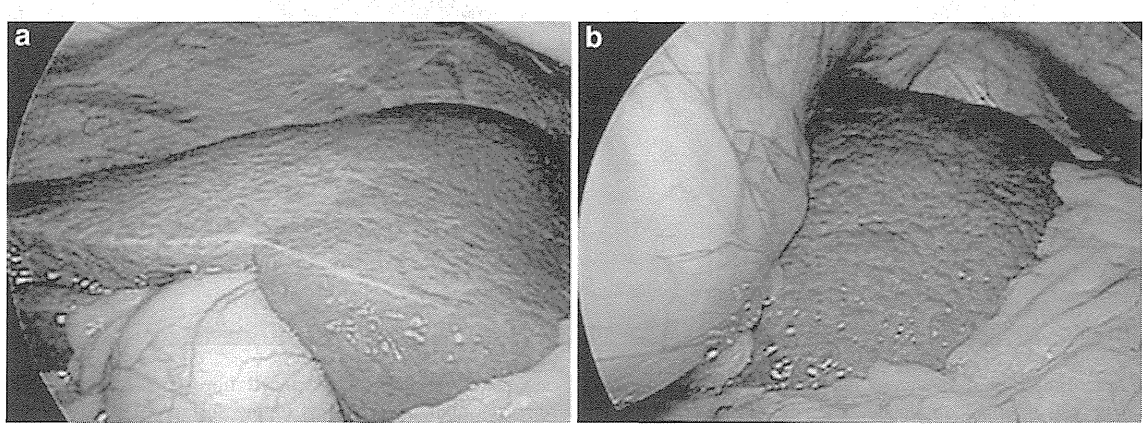

Fig. 2 Conventional laparoscopic image of the liver of the same patient in Fig. 1c. **a** View of the right lobe of the liver. The surface of the liver has diffuse small irregularities. **b** View of the left lobe of the liver. The surface of the liver has diffuse small irregularities and a large nodular area